A LOOK AT DIRECT ARRIVALS

Raul Estevez and Terry Fulp

Success of the Noah deconvolution operator for suppressing water-bottom multiples depends upon one's ability to whiten the seismogram. Previously developed least-squares waveform estimators (Claerbout, SEP-10, and Estevez, SEP-8) are limited to the estimation of short waveforms or their inverses. Unfortunately, in many real data examples, the waveforms tend to be quite long (on the order of 1/2 sec) owing to the source reverberation. Thus, a preprocessing of the data to shorten the signature seems to be necessary if we wish to apply these estimation techniques. The recorded direct arrivals provide some information that might be used to achieve this goal.

The difficulty lies in the delineation and removal of the inherent differences between the recorded horizontal wave and the vertical wave sent into the subsurface. Several physical factors are involved, including the asymmetrical radiation pattern of the source, the antenna response of the cable section, and ghosting effects from the free surface. We intend to discuss some of these effects in a later paper.

To get an understanding of the character of these direct arrivals, we have looked at two different sets of marine data, furnished by two of our sponsors. The first set was collected in the Gulf of Alaska, and the second is from the Grand Banks area off Newfoundland. The important field parameters are presented in Table 1. A description of the direct arrivals as functions of shot point and offset within a gather follows.

In Figs. 1(a) and 2(a), direct arrivals of the near trace of twenty different common shot gathers are shown. The waveforms in general are constant from shot to shot, although there are differences over a larger range. In both data, the bubble reverberation is quite prominent and lengthens the initial pulse to nearly 1/2-sec duration. The higher-frequency ripples that tend to give a doublet appearance seem to be related to the antenna response of the streamer cable.

TABLE 1. Field parameters

Parameter	*Data Set #1*	*Data Set #2*
Location	Gulf of Alaska	Grand Banks
Energy source	Tuned air guns	Tuned air guns
Number of guns	22	Unknown
Gun capacity	1200 in^3	1200 in^3
Source depth	7-10 m	7-8 m
Offset--center airgun array to center near group	238 m	311 m
Group interval	50 m	50 m
Phones/group	30	30
Cable depth	10-14 m	12-17 m
Field filter	8-62 Hz	8-62 Hz
Sampling rate	4 ms	4 ms

Figures 1(b) and 2(b) show approximated inverses of these direct arrivals. The non-causal filters were computed with a standard least-square procedure and were therefore constrained to be somewhat short. Note that for many of the inverses, a significant part of the energy is contained in a small time window near $t = 0$. Although this characteristic is not observed for all the traces, it suggests that better results may be obtained by estimating the inverse source wave forms.

Direct arrivals for a fixed shot and different offsets are displayed in Figs. 3 and 4. Here the shape of the waveforms tends to change, especially in the high-frequency content. The plot does not show true relative amplitudes, which decay very rapidly with offset. Thus a big part of the additional energy at large offset is because of the signal's amplitude reaching the noise level of the trace.

In Figs. 5 and 6, the amplitude spectra of direct arrivals from the near traces of five gathers show little variation in frequency content with shot point. All traces for the first data set are void of frequencies in the

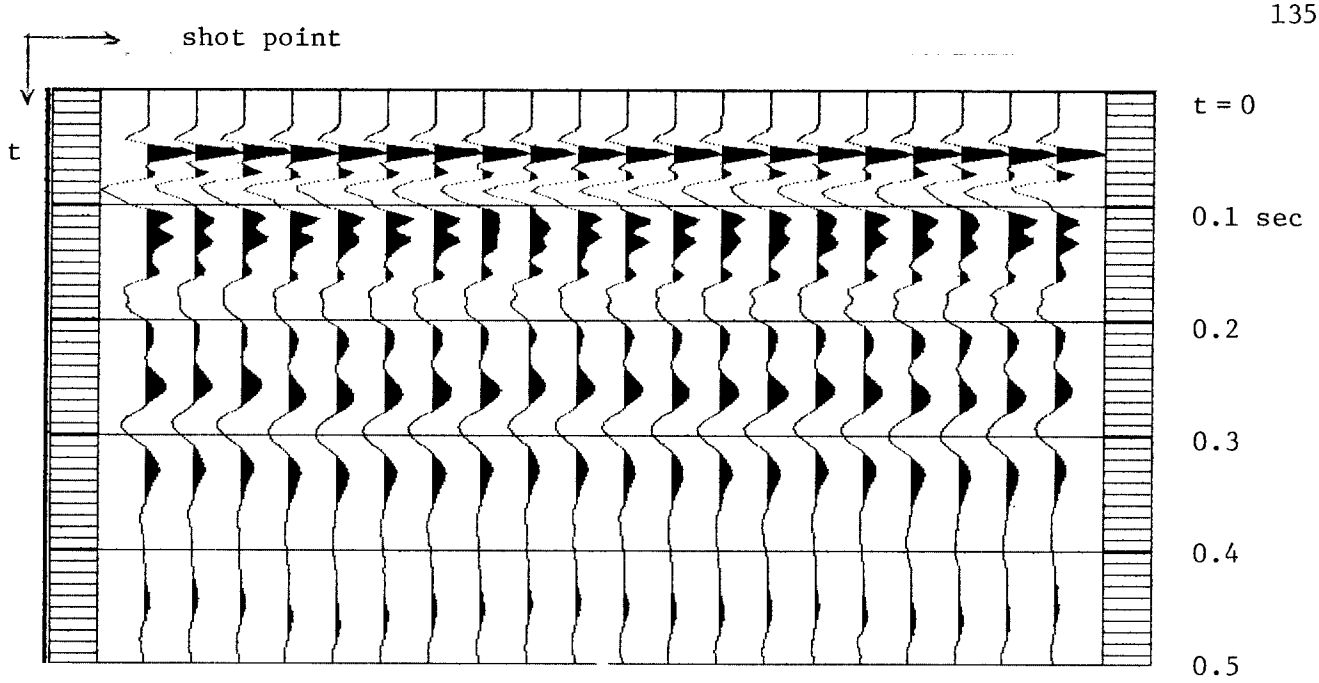

FIGURE 1(a). Direct arrivals as function of the shot point for Data Set #1. The waveforms correspond to the nearest offset trace of 20 different common shot gathers. Zero time was chosen arbitrarily.

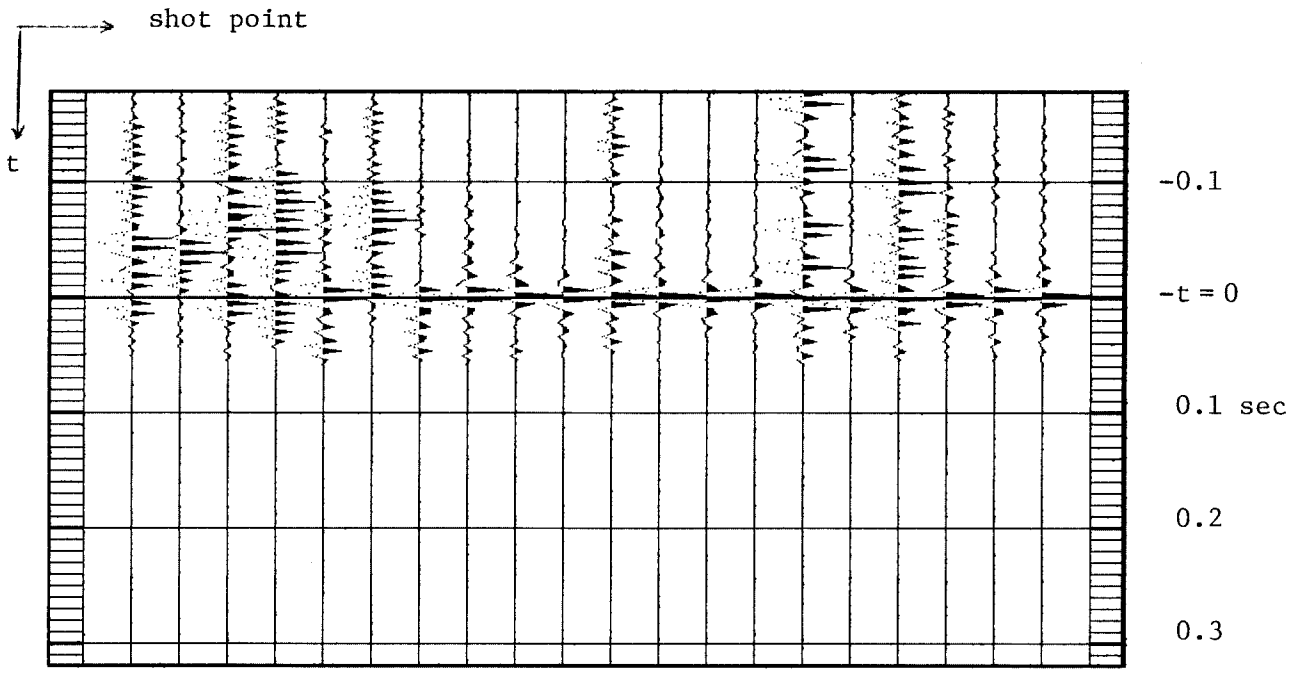

FIGURE 1(b).—Inverse waveforms corresponding to the direct arrivals shown above. A short inverse filter was computed using least squares.

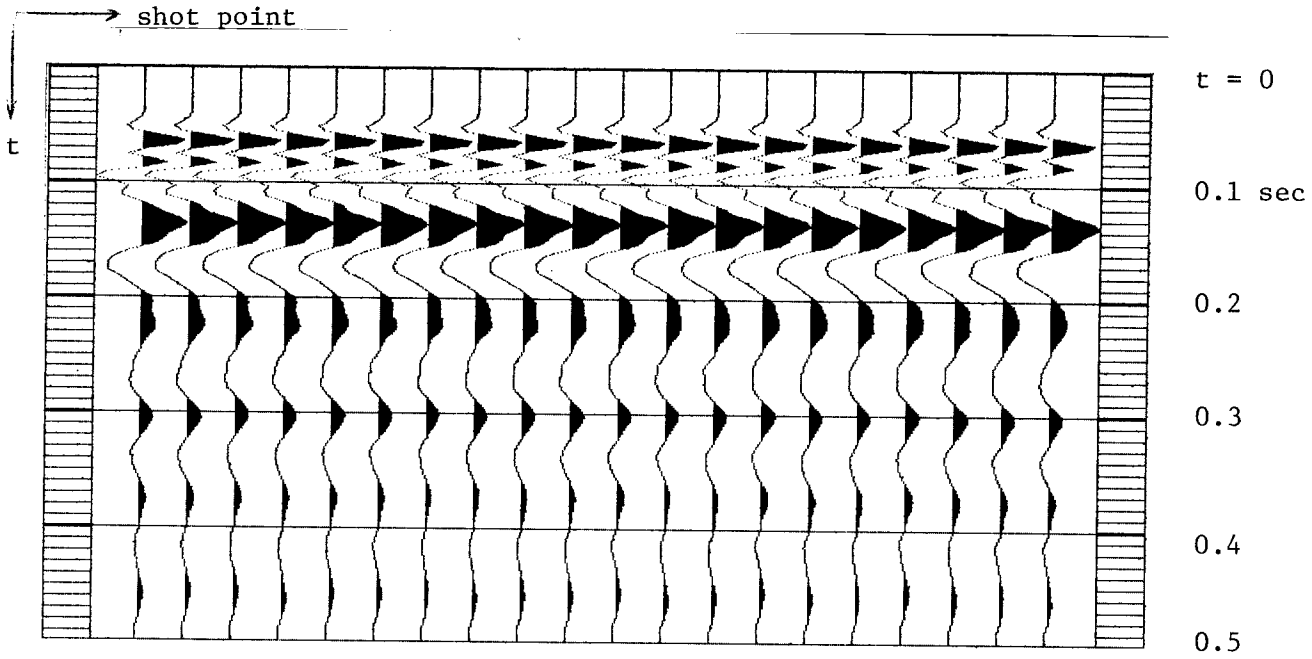

FIGURE 2(a).—Direct arrivals as function of the shot point for Data Set #2. The waveforms correspond to the nearest offset trace of 20 different common shot gathers. Zero time was chosen arbitrarily.

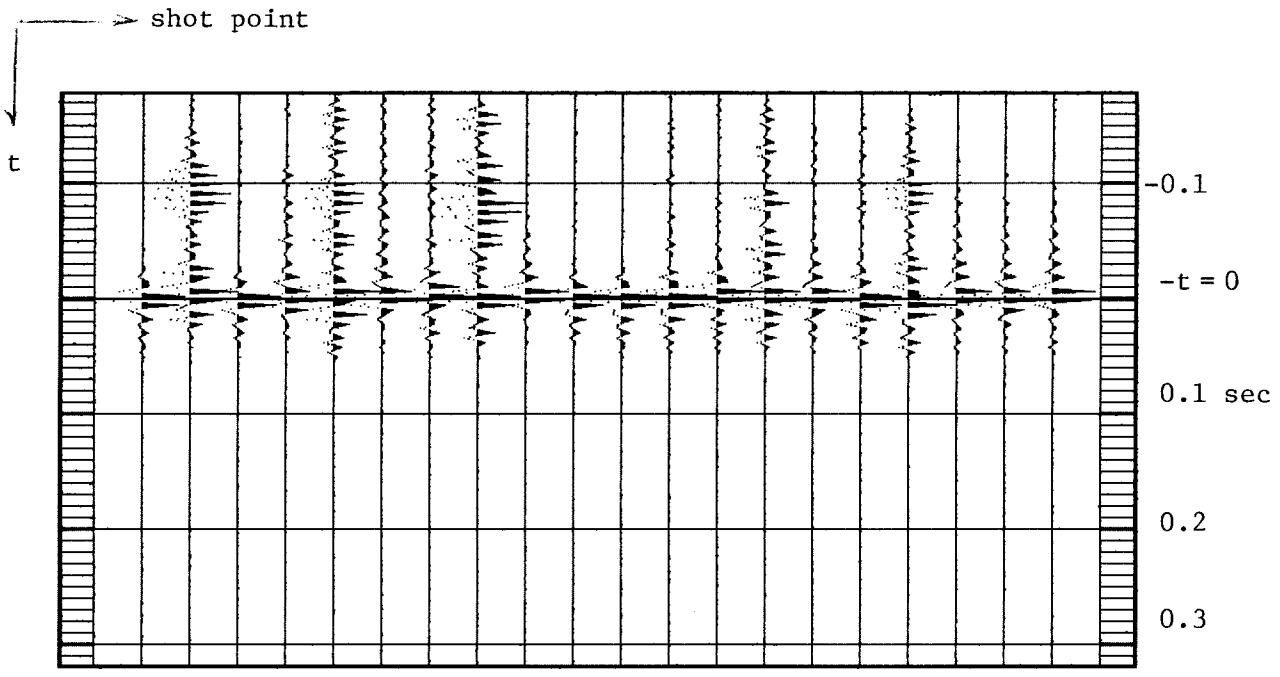

FIGURE 2(b).—Inverse waveforms corresponding to the direct arrivals shown above. A short inverse filter was computed using least squares.

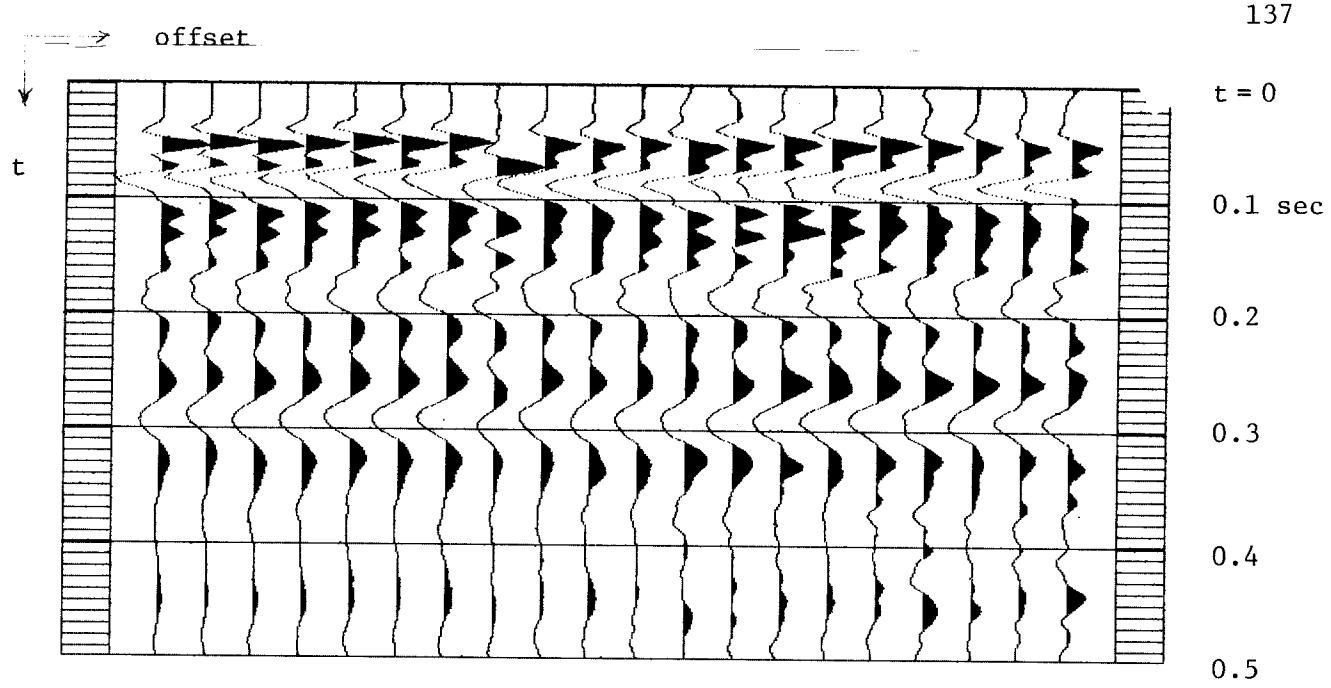

FIGURE 3(a).—Direct arrivals as function of the offset for Data Set #1. The waveforms correspond to the first 20 traces of a common shot gather. The offset increases from left to right. Each trace was scaled separately for display so that relative amplitudes are not preserved. The arrivals were read off the traces and realigned assuming a water velocity of 1460 m/sec.

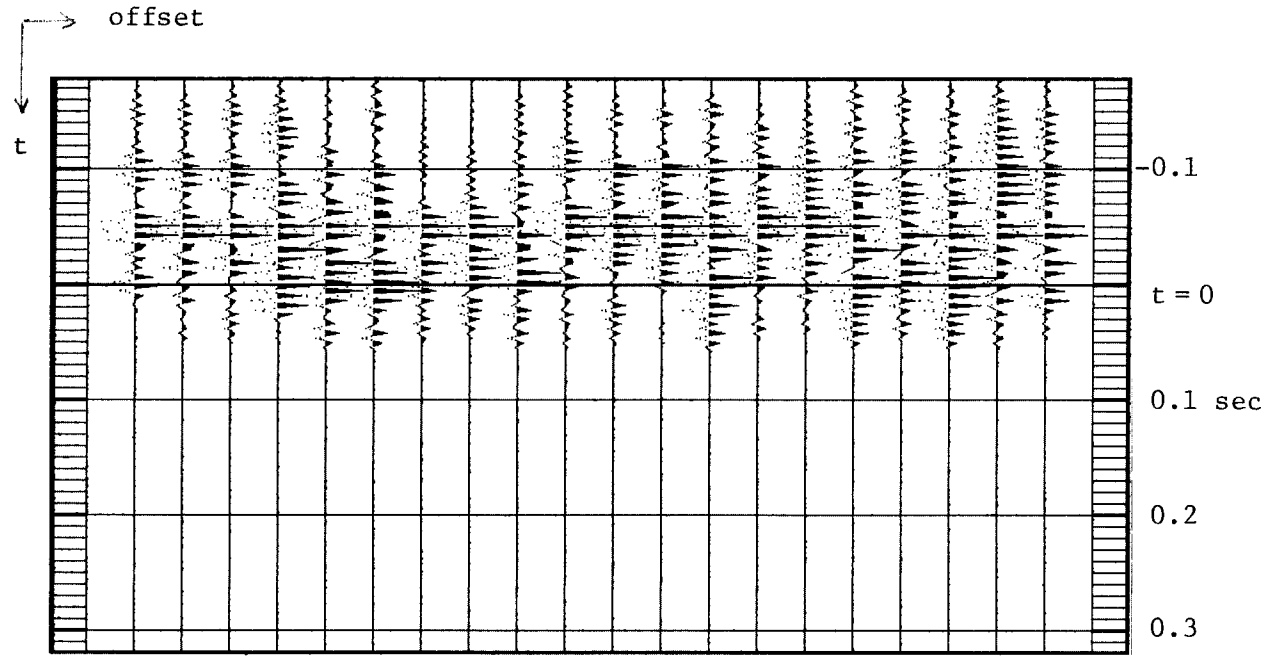

FIGURE 3(b).—Computed inverse waveforms of the above.

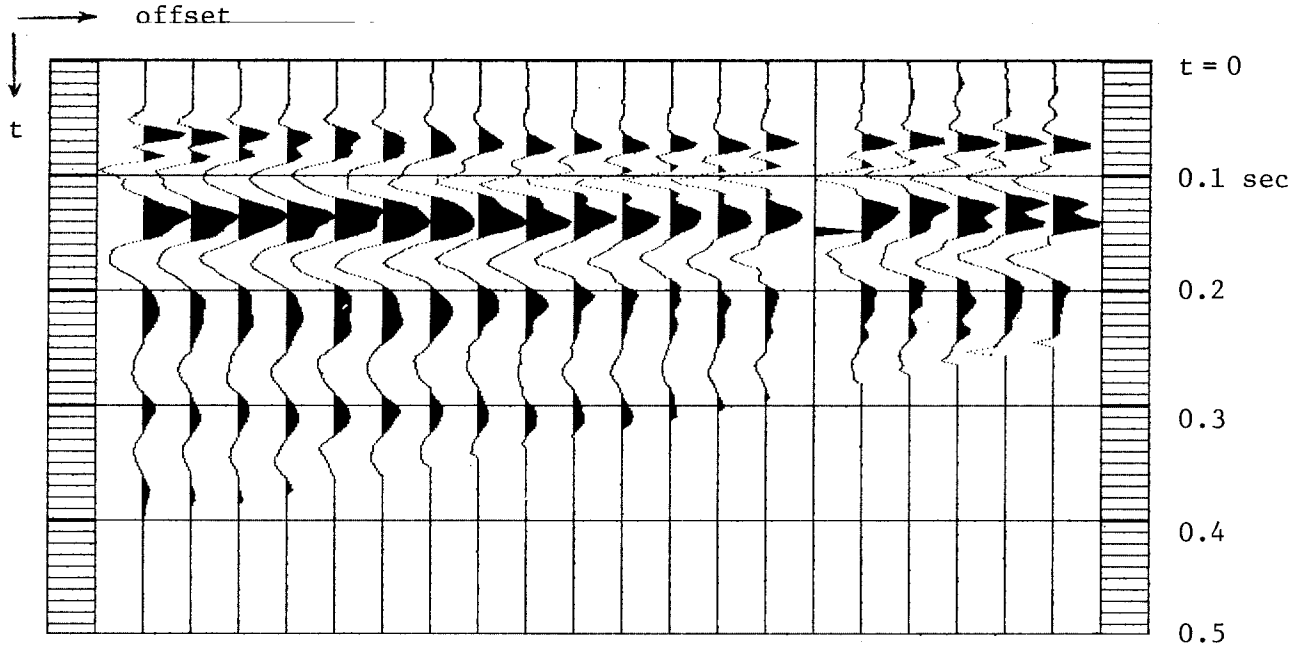

FIGURE 4(a).—Direct arrivals as function of the offset for Data Set #2. The waveforms correspond to the first 20 traces of a common shot gather. The offset increases from left to right. Each trace was scaled separately for display so that relative amplitudes are not preserved. The arrivals were read off the traces and realigned assuming a water velocity of 1460 m/sec. Since the water depth was not large enough, the sea-floor arrival interfered with the direct arrival and an abrupt offset-dependent cutoff was applied.

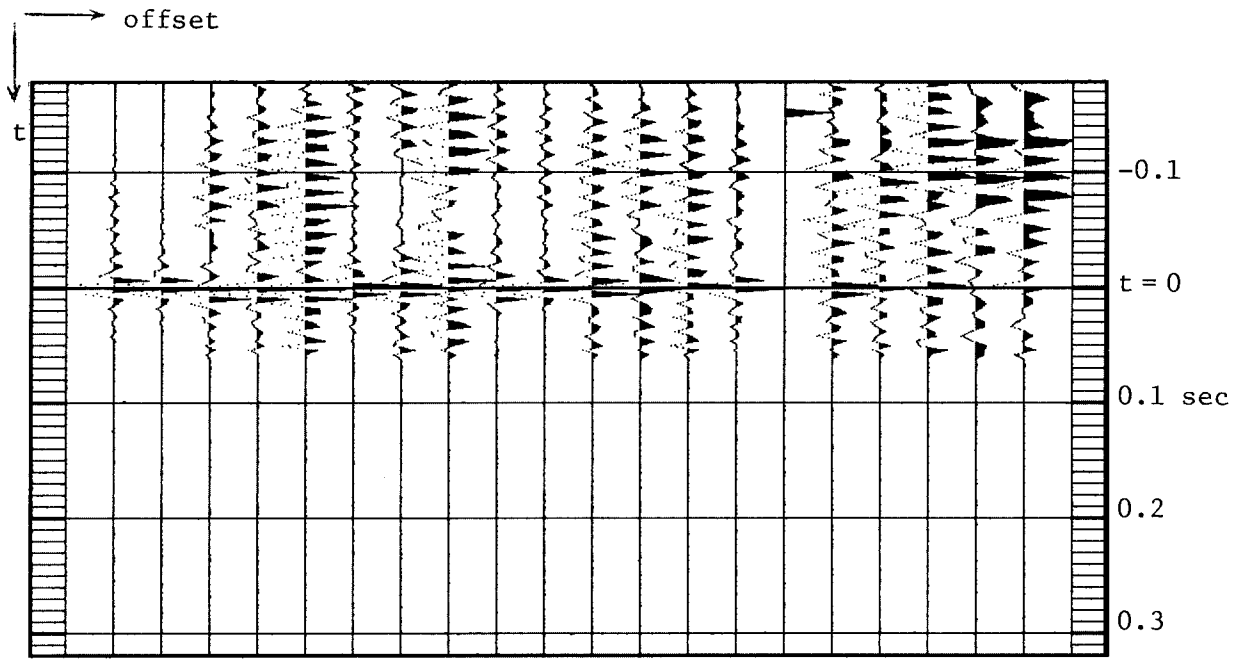

FIGURE 4(b).—Computed inverse waveforms of the above.

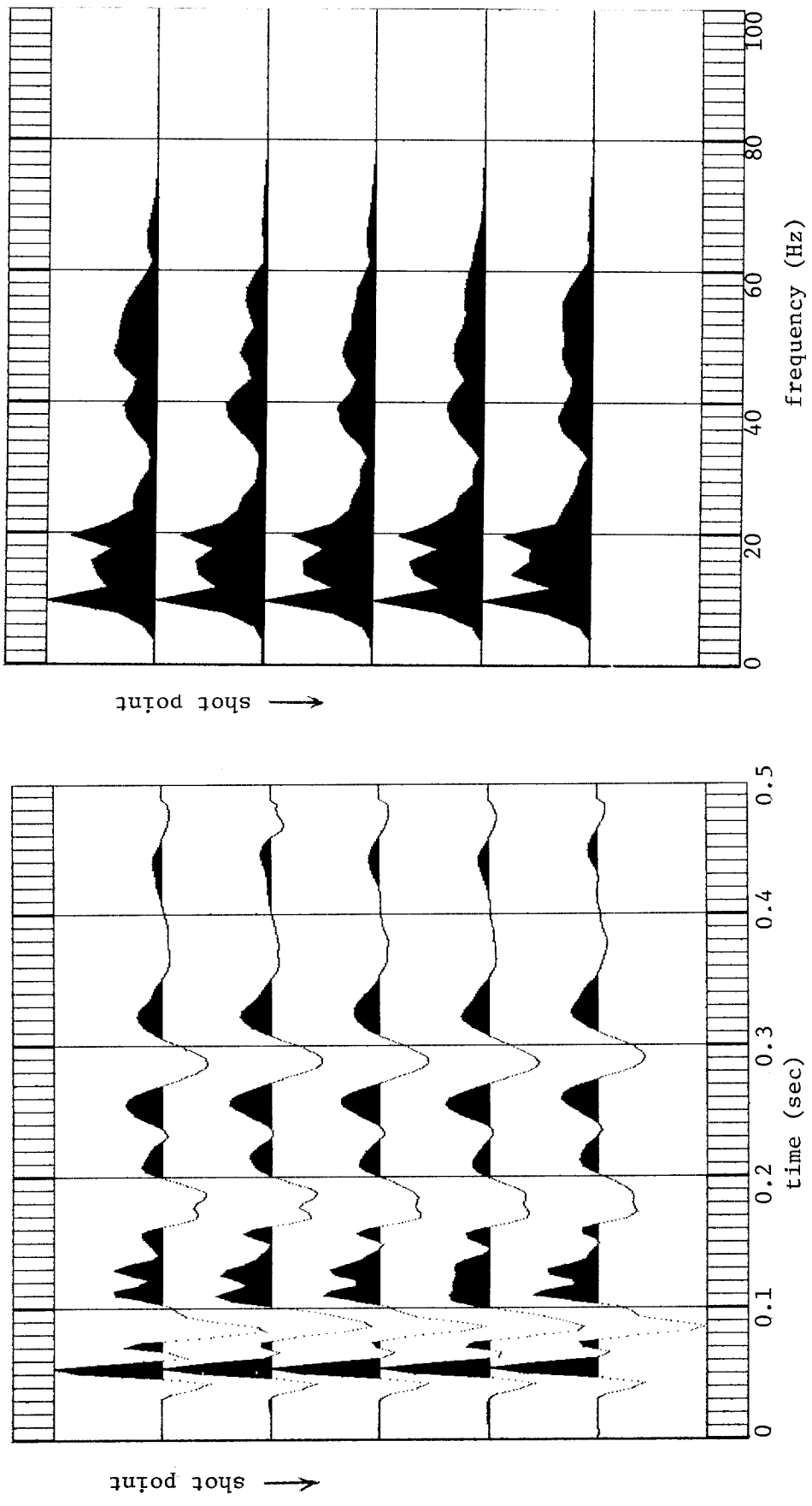

FIGURE 5.—Direct arrivals and their computed amplitude spectra from the near trace of five gathers of Data Set #1 (each 100-m apart). Timing lines are at 0.01 sec and frequency lines every 2 Hz. Only the positive frequencies are shown out to 100 Hz (Nyquist frequency is 125 Hz). Each trace and each spectrum has been normalized to its maximum for display.

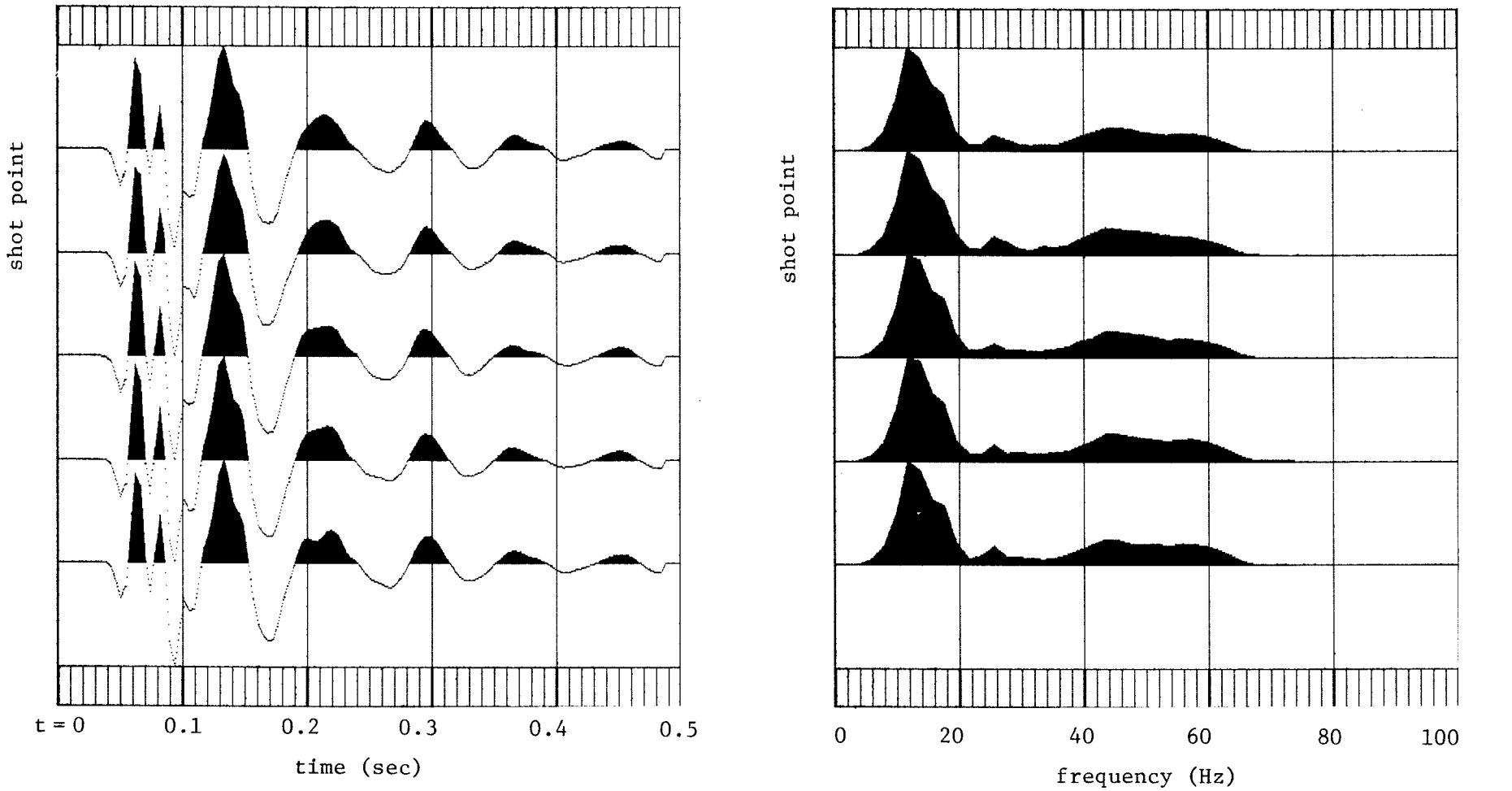

FIGURE 6. Direct arrivals and amplitude spectra from the near trace of five gathers of Data Set #2 (each 100-m apart). Timing and frequency lines as in Fig. 5.

28-34 Hz range. This seems to be the result of the integration effect of the finite number of recorders making up a single channel. A simple calculation with a water velocity of 1500 m/sec and a wavelength of 50 m (the length of the geophone group) confirms this. Likewise, the data of Fig. 6 have little energy in the same band. We expect that the gross differences between the two data sets (e.g., at 20 Hz) are due to a real difference in the character of the sources.

Figures 7 and 8 show the spectra as functions of offset within a gather. Again we see the antenna effect of the cable section, but we also note a scattering of the "holes" with offset. We attribute this to the complicated bubble pulse generated by the source reverberation. This variation suggests some averaging of the spectra over offset if we want to relate the information in direct arrivals to stacked sections.

Finally, spectral factorization of some of the traces is shown in Figs. 9 and 10. As we know, any signal can be factored uniquely into a minimum phase component and an all-pass filter. Both components were computed using Claerbout's spectral factorization routine (*Fundamentals of Geophysical Data Processing*, p. 62). The minimum phase component is very long and, except for the beginning, is almost a shifted version of the direct arrival. This would indicate that in both data the signature is very close to being minimum phase and accordingly, the all-pass component is very short and localized. This pattern tends to deteriorate with offset, however.

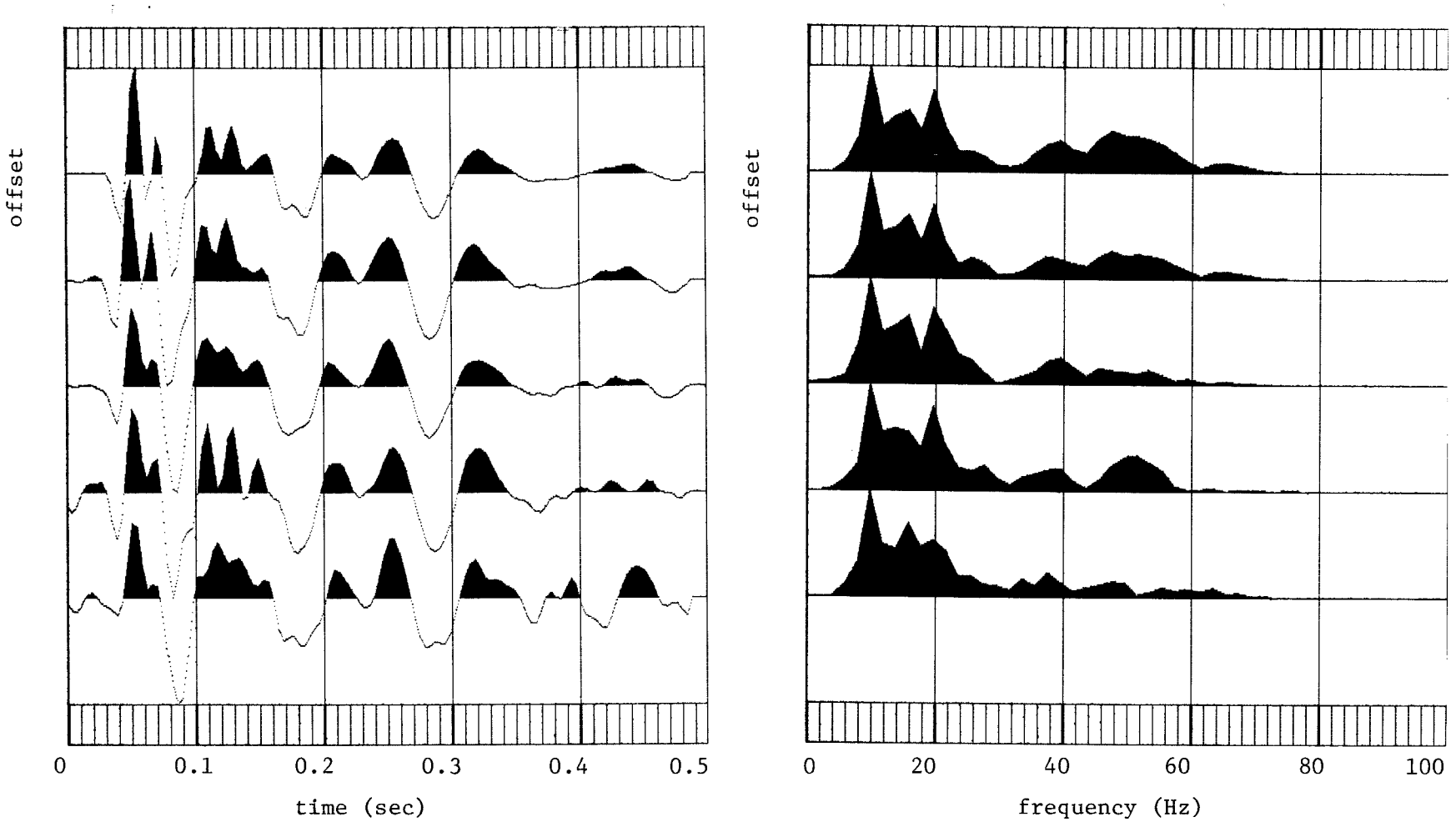

FIGURE 7.—Direct arrivals and amplitude spectra from a single gather of Data Set #1. Every 4th trace is shown beginning with the near trace (each is 100-m apart).

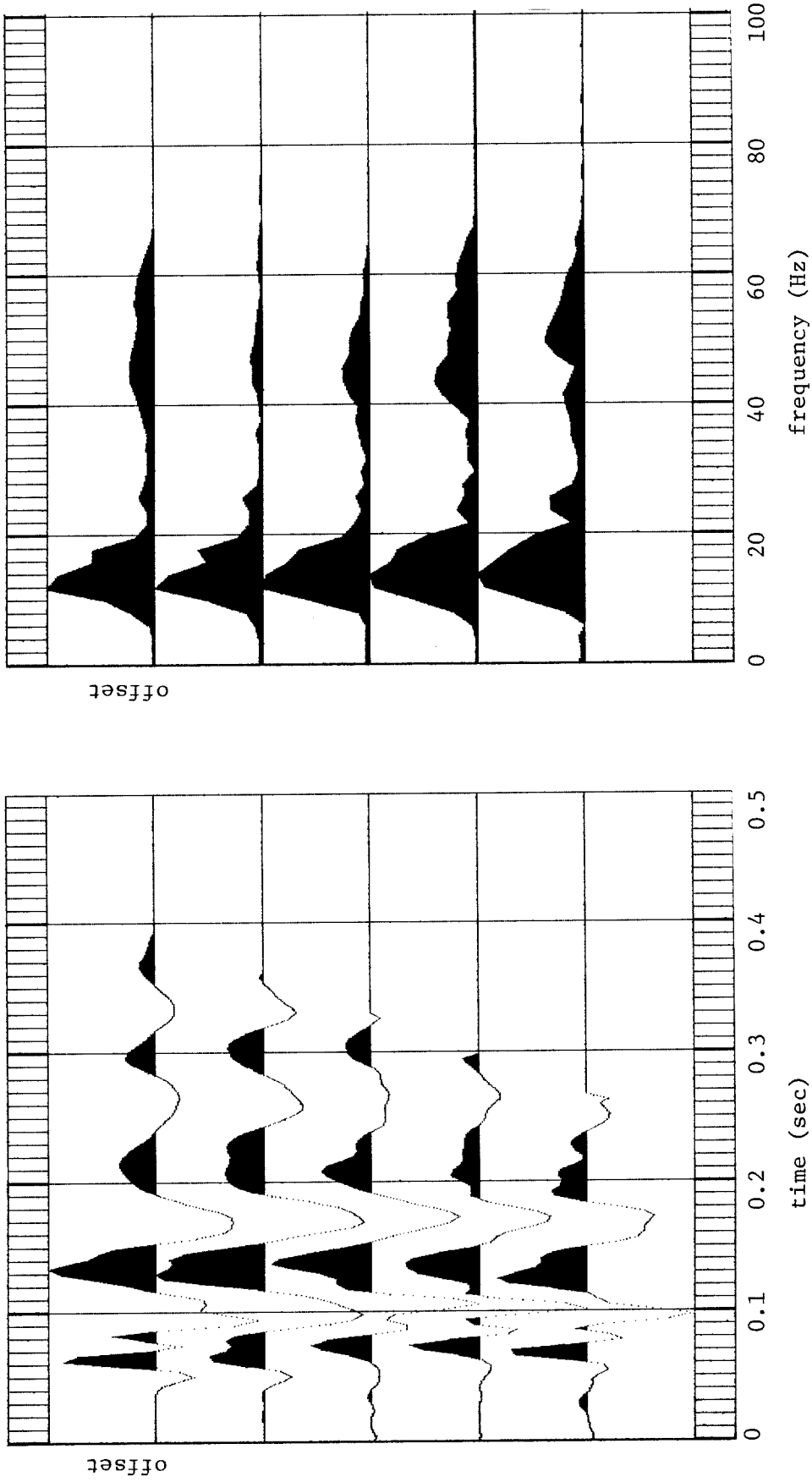

FIGURE 8.—Direct arrivals and spectra from a single gather of Data Set #2. Every 4th trace is shown beginning with the near trace. (Each is 100-m apart.) Timing and frequency lines as before.

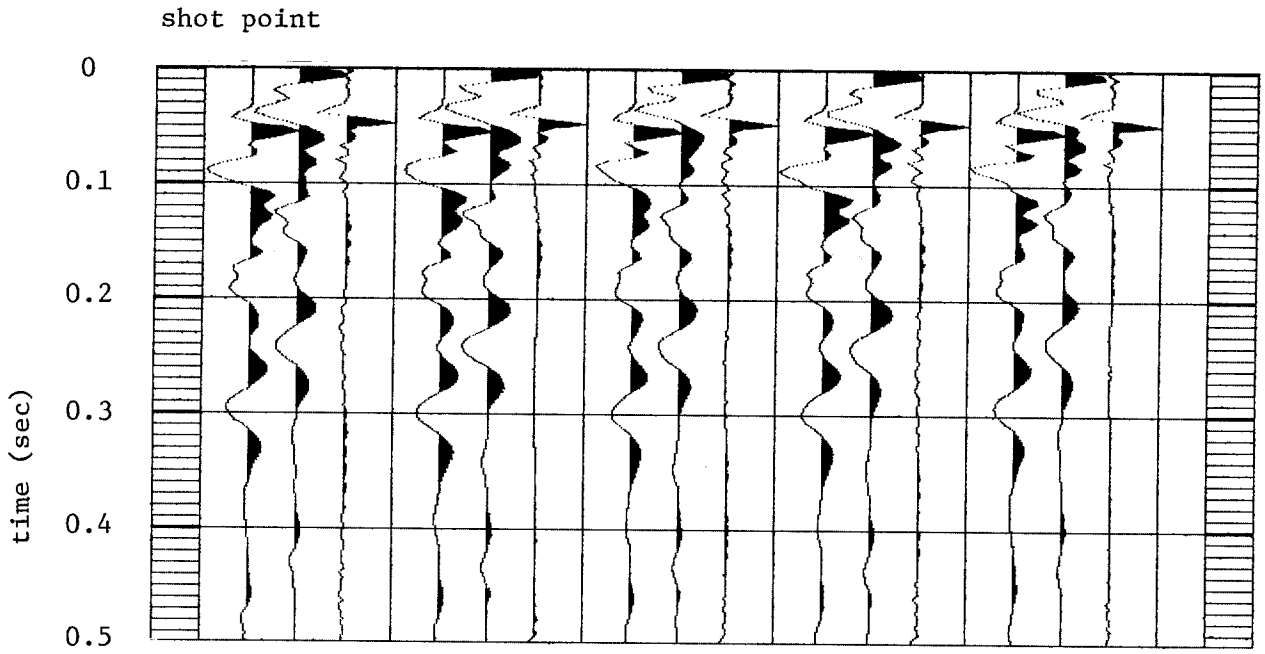

FIGURE 9(a).—Minimum phase and all pass components of the direct arrivals of Data Set #1 as a function of shot point. From left to right: the trace, the minimum-phase component, and the all-pass filter. The direct arrivals were picked up every four traces in relation to Fig. 1(a), so that they correspond to traces 1, 5, 9, and 17.

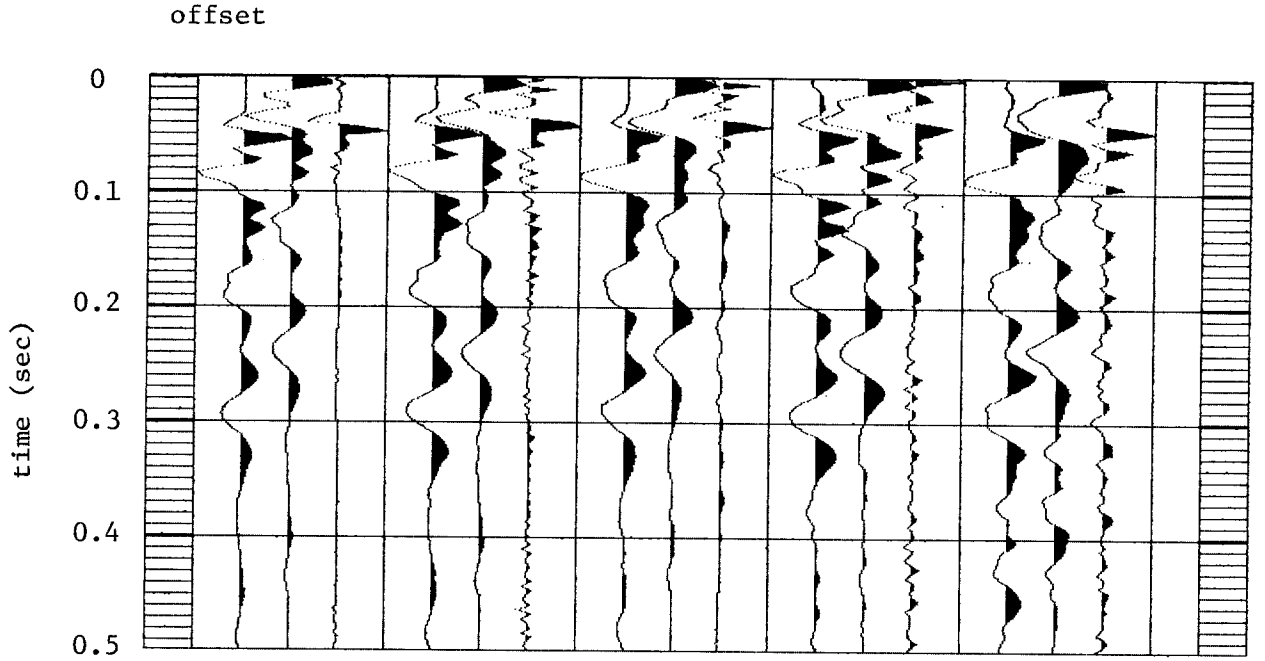

FIGURE 9(b).—Minimum phase and all-pass components of direct arrivals of Data Set #1 for different offsets within a gather. As above, they are traces 1, 5, 9, and 17 of Fig. 3(a).

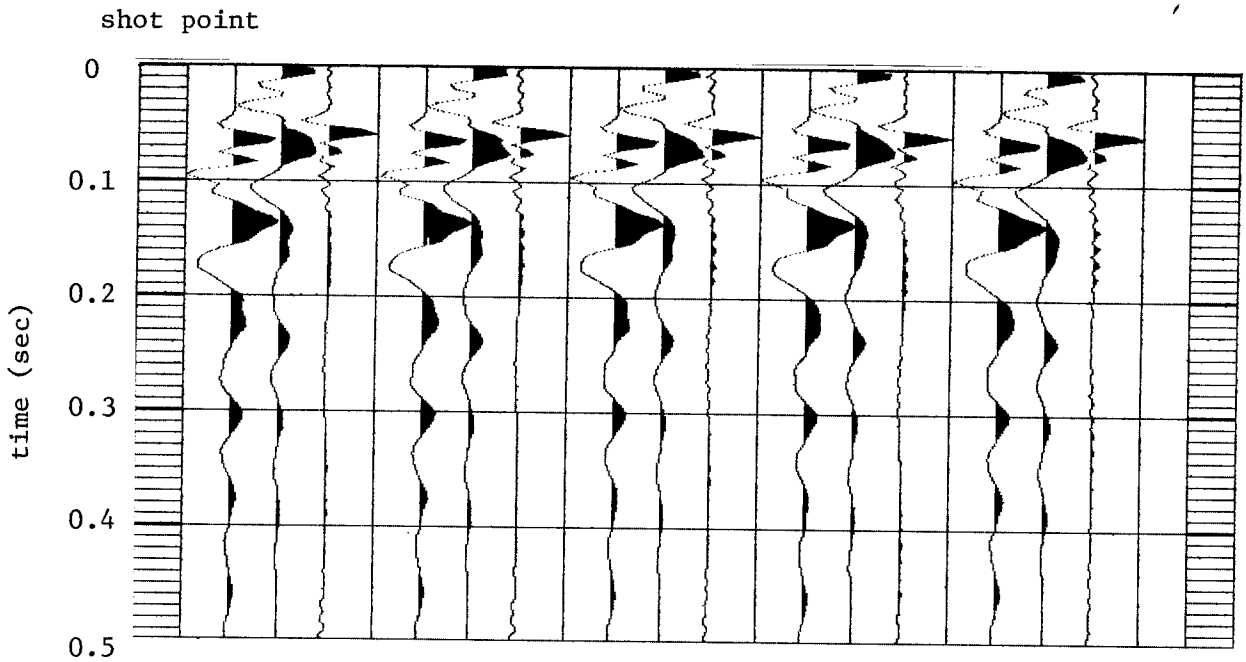

FIGURE 10(a).—Minimum phase and all-pass components of Data Set #2 as a function of offset.

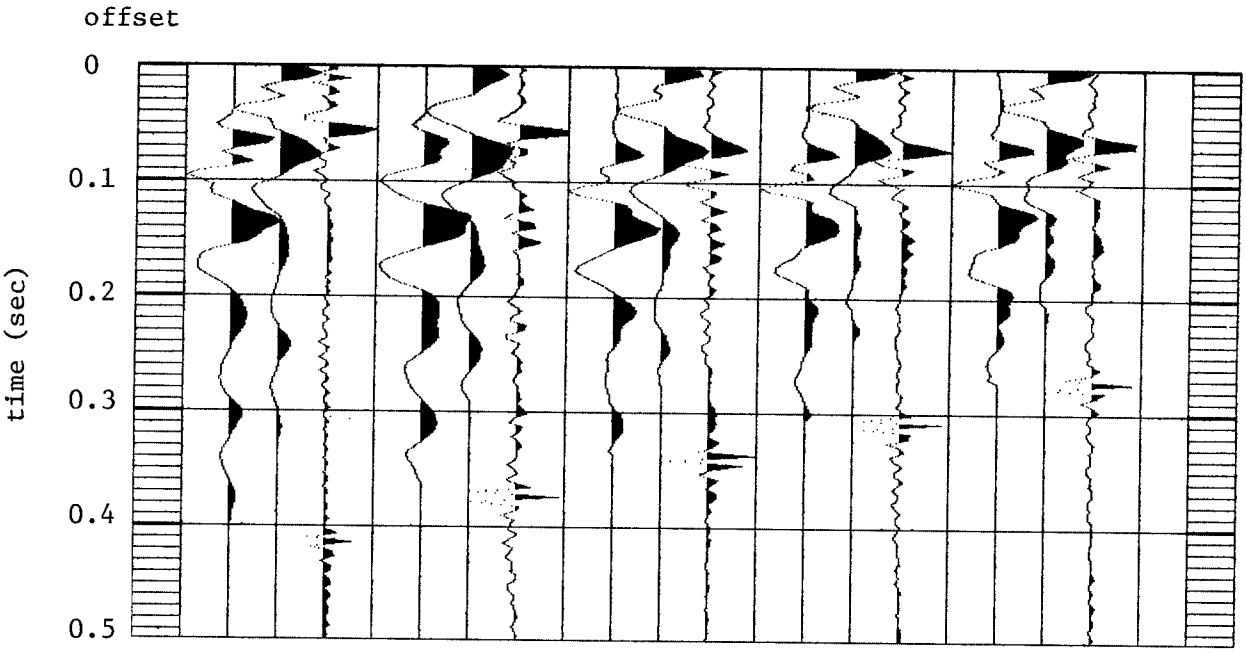

FIGURE 10(b).—Minimum phase and all-pass components of Data Set #2 for different offsets within a gather. The peaks toward the ends of the all-pass filters are artifacts of the abrupt window applied to the direct arrivals.